

Potential Applications and Current Limitations

Makoto Higuchi and Takaomi C. Saido

Laboratory for Proteolytic Neuroscience, RIKEN Brain Science Institute, 2-1 Hirosawa, Wako, Saitama 351-0198, Japan.
Email: mhiguchi@brain.riken.jp, saido@brain.riken.jp

Introduction

Alzheimer's disease (AD) is the most common cause of senile dementia, and afflicts approximately 10 million elderly people in the world. This devastating disorder is neuropathologically characterized as brain amyloidosis, which means that there is a progressive accumulation of protein aggregates with a β -pleated sheet structure [1]. Extracellular and intraneuronal amyloid deposits, which are referred to, respectively, as senile plaque and neurofibrillary tangle, are known as pathological hallmarks of AD [1]. Moreover, major constituents of these amyloid lesions have been implicated in the onset and progression of AD.

Senile plaques are composed of self-assembled filaments of amyloid β peptide ($A\beta$), and genetic mutations which induce overproduction of $A\beta$ have been found to cause familial AD [2]. Neurofibrillary tangles are comprised of abnormal tau protein filaments, and recent discoveries of tau gene mutations in kindreds of familial non-AD dementias have led to the hypothesis that pathological alterations of tau proteins alone can lead to neurodegenerative conditions [3]. Current clinical workup for AD does not allow definite diagnosis of this disease in living patients due to lack of tools to assess AD-specific pathologies prior to death. Since the emergence of amyloid aggregates precedes clinical onset of AD by 10 - 20 years [4], detection of amyloidosis in the brain in vivo is likely to permit highly precise diagnosis of AD at a preclinical stage on a neuropathological basis.

Amyloid-Binding Compounds as Diagnostic Probes

To date, a number of investigations by independent research groups have demonstrated the utility of noninvasive imaging technologies in the visualization of amyloid lesions accumulating in AD patients and/or animal models of AD. The progress of these studies has been greatly facilitated by the development of brain-penetrating, amyloid-binding molecules, which can be used as imaging tracers. It is well known that several fluorescent dyes, such as Congo red and thioflavin-T (Fig. 1), strongly bind to β -pleated sheet structures and are useful in histochemical examinations for neu-

ropathological diagnosis of AD. However, due to electric charge or molecular size, these "classical" amyloid ligands do not cross the blood-brain barrier (BBB) and enter brain tissue when administered intravenously. Thus, derivatives of Congo red and thioflavin-T with reduced molecular mass or neutral charge have been generated and tested as candidate probes for AD amyloid.

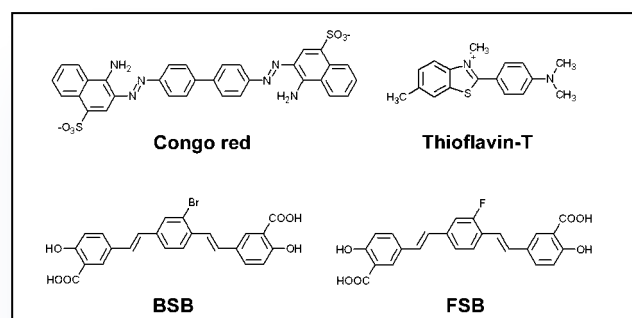


Fig. 1: Chemical structures of amyloid-binding fluorescent dyes.

One of the compounds which was demonstrated to bind to senile plaques in vivo after intravenous administration was (*trans, trans*)-1-bromo-2,5-bis-(3-hydroxycarbonyl-4-hydroxy)styrylbenzene (BSB), a styrylbenzene analog of Congo red (Fig. 1). BSB is a fluorescent dye with a high affinity for a β -sheet structure. After intravenous injection of BSB, strong fluorescence signals were detected on amyloid plaques in brains of transgenic mice overexpressing the amyloid precursor protein (APP), from which $A\beta$ is produced by proteolytic cleavages [5]. Moreover, it has been shown that replacement of the bromine atom in BSB with radioactive iodine may provide an amyloid tracer suitable for single-photon-emission computed tomography (SPECT). Since the distribution of such radioligands in the brain after intravenous injection ranged from only 0.15% to 0.3% of injected dose, their pharmacokinetic characteristics may not suffice for radiological imaging [6].

¹⁹F-MRI of a Transgenic Mouse Model of AD

We have recently developed a new amyloid-binding analog of BSB with a fluorine instead of bromine substituent. The resulting compound, (*trans, trans*)-1-fluoro-2,5-bis-(3-hydroxycarbonyl-4-hydroxy)styrylbenzene (FSB), was found to have even better fluorescence properties and higher affinity for $A\beta$ amyloid when compared with BSB [7]. Ex vivo his-

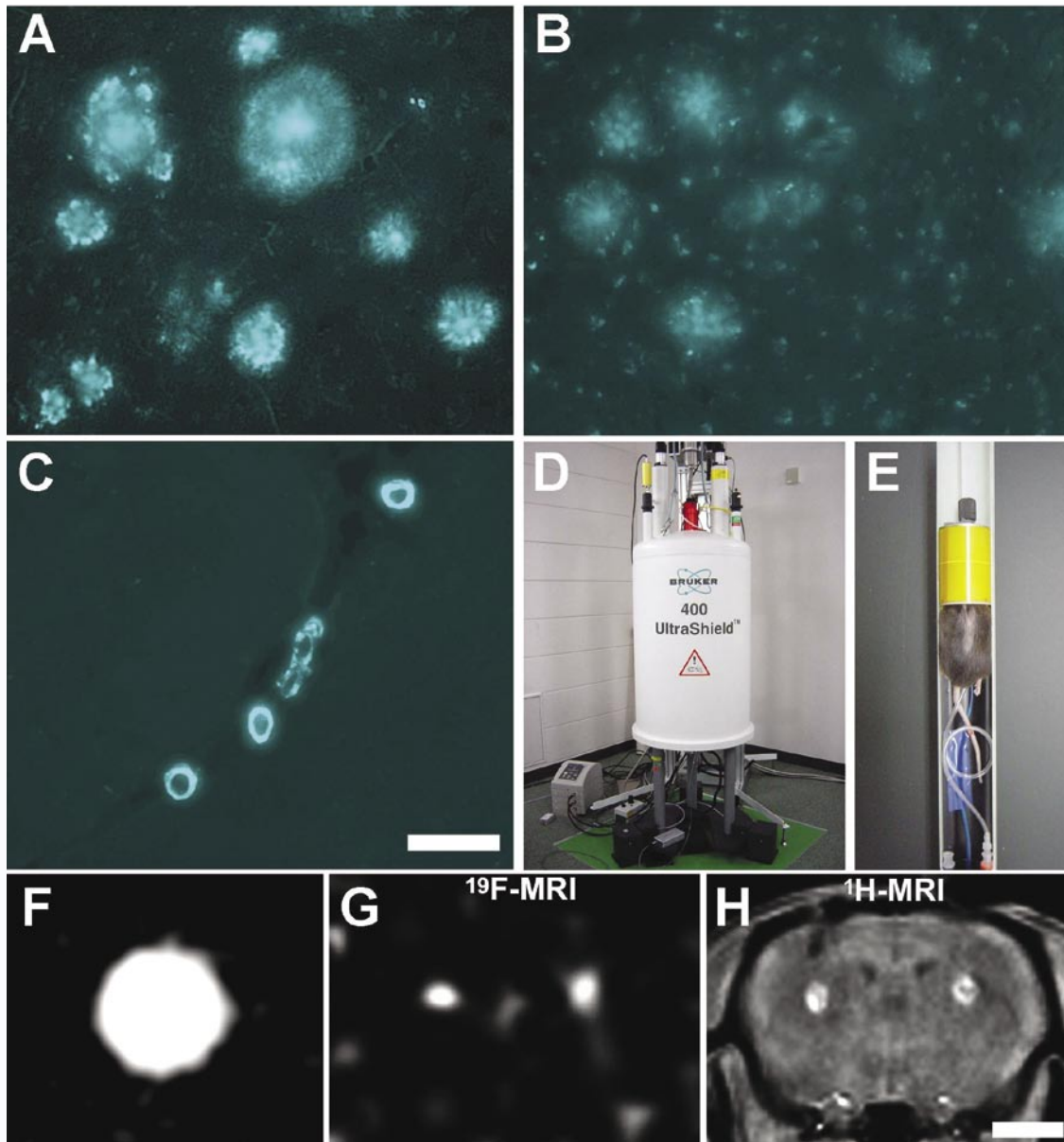


Fig. 2: Application of FSB for the detection of senile plaques in APP transgenic mice. Fluorescence microscopy detects more intensive staining of senile plaques with intravenously injected FSB (A) compared to BSB (B). The staining of cerebrovascular amyloid was similar for FSB (not shown) and BSB (C) after intravenous injection. The white scale bar corresponds to 100 μ m in images A-C. D: 9.4 T wide-bore magnet system used for microimaging (Avance 400). E: Microimaging probe specifically designed for in vivo studies of the mouse head. F: Transverse ¹⁹F-NMR image of a 1% FSB solution in a test tube phantom, acquired using a 3D-RARE spin-echo sequence as described in the text. G: Transverse ¹⁹F-NMR image acquired from mouse brain in vivo after topical injection of FSB into the bilateral basal ganglia (bright spots). H: Corresponding T₁-weighted gradient-echo ¹H-NMR image (scale bar = 2 mm for images F-H).

tology of brain sections from APP transgenic mice revealed that intravenously administered FSB accumulates in intracranial amyloid plaques more abundantly than BSB, while the binding of FSB to cerebrovascular amyloid deposits was comparable to that of BSB (Figs. 2A-2C). These observations suggest that FSB crosses the BBB more efficiently than BSB, presumably due to the smaller size of the fluorine atom compared to bromine. With its built-in ¹⁹F label FSB allows the application of fluorine-MRI for studying brain amyloid. Since the receptivity of ¹⁹F is 83% relative to ¹H and endogenous fluorine occurs at only very low levels in biological tissues as fluoride anion, tracer imaging without background signals is possible in principle. Therefore, we have investigated the applicability of FSB for the visualization of senile plaques in APP transgenic mice by fluorine-MRI.

In order to detect ¹⁹F NMR signals in the mouse brain in vivo, we employed a Bruker AVANCE 400 wide-bore spectrometer (Fig. 2D) with imaging accessories and an actively shielded Micro2.5 gradient system (25 mT/m/A) with 40-mm inner diameter. The microimaging probe with animal handling capabilities employed a 25-mm bird-cage resonator which was double-tuned to ¹H (at 400 MHz) and ¹⁹F (at 367.5 MHz) (Fig. 2E). A test tube containing 1% FSB in DMSO gave a strong ¹⁹F signal within one minute with a 3D RARE spin-echo sequence (data matrix = 32 × 32 × 8 voxels, field of view = 20 × 20 × 16 mm, voxel dimensions = 0.31 × 0.31 × 2 mm, spectral width = 25 kHz, TR/TE = 2000/4.2 ms, RARE factor = 32), indicating that the T₂ relaxation time of FSB in solution was sufficiently long (Fig. 2F). A similar protocol for image acquisition was also

applied to anesthetized mice that underwent an intracranial injection of 2.5% FSB. It was possible to image ^{19}F at the injection sites within 90 min (**Figs. 2G & 2H**) [8].

Subsequently, 500 μl of a 0.2% FSB solution in phosphate-buffered saline containing 10% DMSO was intravenously infused into APP transgenic mice (age: 12-25 months) over a period of 150 min (total FSB dose: 1 mg or ca. 20 mg/kg). 3D-RARE ^{19}F -MR images were acquired in the following 120 min using parameters similar to those for the phantom experiments (data matrix = $32 \times 32 \times 8$ or $64 \times 64 \times 8$ voxels). The mice were anesthetized with pentobarbital, and the depth of anesthesia was monitored and maintained during the tracer infusion and MR scans.

The ^{19}F images showed hyperintensity foci primarily in the hippocampus and entorhinal cortex of the transgenic mice (**Figs. 3A & 3C**), and these foci corresponded to sites of accumulation of FSB in $\text{A}\beta$ plaques, as confirmed by direct microscopic examination of the dissected brains immediately after MRI (**Figs. 3E & 3F**). In addition, the intensity of ^{19}F -MR signals correlated well with the abundance of $\text{A}\beta$ plaques, as quantified by fluorescence microscopy (**Fig. 4**) [8]. In view of the relative sizes of the image voxels and typical senile plaques (< 150 μm in diameter), it is likely that ^{19}F -MRI mainly captured clusters of plaques but not an isolated single lesion. It was also apparent that ^{19}F -MRI could detect amyloid deposits only when their occupancy reached 5-10% of the target brain areas [8]. The signal-to-noise ratio with the 3D-RARE sequence was found to be highly dependent on the local B_0 field homogeneity, and ^{19}F signals were not efficiently obtained if shimming was less than optimal.

Detection of Brain Amyloid by ^1H -MRI

Recent high-field ^1H -MRI technologies have demonstrated visualization of isolated senile plaques in animal models of AD [9]. We also conducted in vivo ^1H -MR detection of amyloid lesions in anesthetized APP transgenic mice using a T_2 -weighted 2D-RARE sequence (matrix = 256×512 , field of view = 20×20 mm, nominal in-plane resolution = 78×39 μm , slice thickness = 500 μm , TR/TE =

3000/4.6 ms, RARE factor = 64, 70 averages in 42 min). As in previous investigations, large plaques (50 - 150 μm in diameter) were visualized as hypointensity lesions with T_2 weighting (**Fig. 3B**). This ^1H -MRI contrast effect was even more evident in ex vivo brain scans performed postmortem (**Fig. 5**) [8].

The shortening of proton T_2 relaxation times in amyloid deposits is attributed to the presence of plaque-associated iron. Therefore, T_2 -weighted ^1H -MRI is capable of mapping brain amyloid without contrast agents. However, the specificity of this imaging protocol may be inferior to tracer-aided amyloid visualization, since other brain pathologies, such as microhemorrhages, can result in similar reductions in T_2 .

Research results have provided evidence that gadolinium-labeled amyloid ligands can enhance the contrast for detecting senile plaques with T_1 - and T_2 -weighted ^1H -MRI [11,12]. The self-aggregating nature of $\text{A}\beta$ peptide enables gadolinium-labeled $\text{A}\beta$ to bind to amyloid plaques, and conjugation of the ligand with putrescine facilitates its transfer through the BBB.

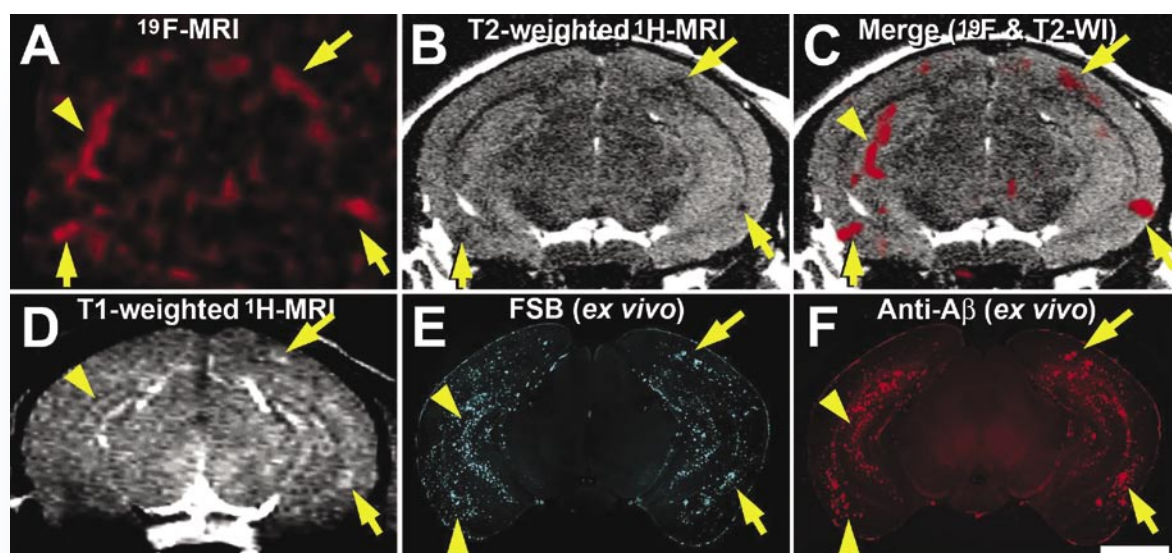


Fig. 3: Detection of senile plaques in an APP transgenic mouse in vivo after intravenous administration of FSB. **A:** In vivo ^{19}F -MRI shows signal intensity (red) from FSB primarily in the cortex (arrows) and hippocampus (arrowhead). **B:** T_2 -weighted ^1H -MRI obtained directly after ^{19}F imaging shows hypointensity foci in the cortex (arrows). **C:** Superposition of the ^{19}F (A) and ^1H (B) images. **D:** T_1 -weighted gradient-echo ^1H -MRI performed after ^{19}F imaging. Hyperintensity areas are found in the cortex (arrows) and hippocampus (arrowhead). Ex vivo histological examination of a brain section from the same mouse correlates high levels of FSB (**E**) with $\text{A}\beta$ plaques (**F**). The arrows correspond to the positions marked in the MR images (scale bar = 2 mm).

It is of interest that FSB also appears to behave as a contrast agent for ^1H -MRI. Intracranially injected FSB resulted in a local increase in signal intensity in T_1 -weighted gradient-echo (GE) ^1H -MRI (**Fig. 2H**, matrix dimensions = 128×128 , field of view = 20×20 mm, nominal in-plane resolution

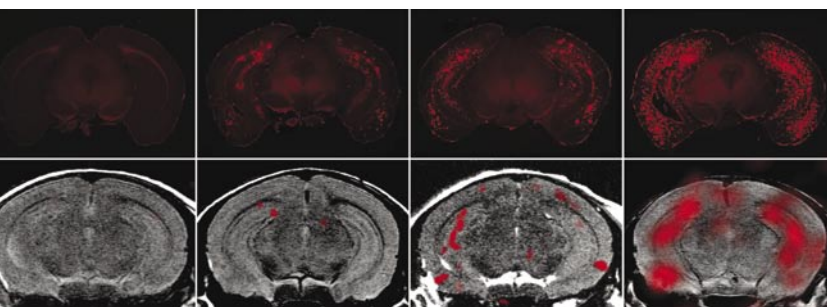


Fig. 4: Correlation between fluorescence microscopy for histological detection of A β plaques ex vivo (top row) and the in vivo ^{19}F -MRI signal intensity from FSB (red, bottom row), overlaid on the ^1H -MRI. Brain amyloid levels are very low in the normal mouse but increase progressively with age in the APP transgenic mouse.

= $156 \times 156 \mu\text{m}$, slice thickness = $500 \mu\text{m}$, TR/TE = 250/1.8 ms, flip angle = 85° , total imaging time = 5 min). The contrast of senile plaques in a similar imaging protocol (matrix dimensions = 128×256 , nominal in-plane resolution = $156 \times 78 \mu\text{m}$, total imaging time = 10 min) was enhanced to some extent after intravenous administration of FSB (**Fig. 3D**) [8]. However, plausible mechanisms for these effects remain to be discovered, and it must be noted that the GE pulse sequence is susceptible to changes in cerebral blood flow.

Conclusion

Visualization of brain amyloid in neurodegenerative disorders has attracted growing attention since it offers the potential of noninvasive neuropathological assessment in vivo and would be useful for monitoring the emerging disease-modifying treatments of AD and related illnesses [13]. After the application of BSB for in vivo amyloid detection was reported [5], diverse amyloid ligands were tested for PET and SPECT studies. Among these tracers, ^{11}C -labeled 6-hydroxy-benzothiazole-aniline (also known as Pittsburgh Compound-B) is the most extensively evaluated for PET examination of human subjects and has been proven to accurately discriminate between aged normal controls and AD patients [14]. On the other hand, high-field, high-resolution MRI is currently the only method

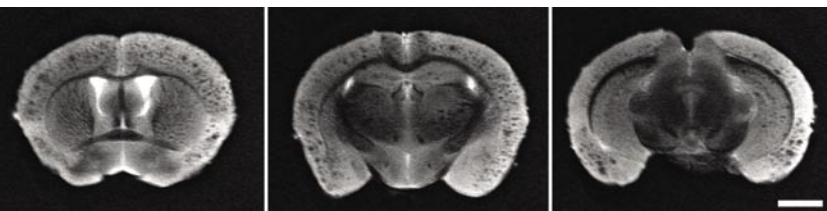


Fig. 5: T_2 -weighted ^1H -MRI of an APP transgenic mouse brain ex vivo (postmortem) showing abundant amyloid plaques as hypointensity foci in the cortex and hippocampus (scale bar = 2 mm).

for noninvasive visualization of individual senile plaques, permitting diagnostic approaches free of the safety and exposure constraints associated with radioactive materials. However, the specificity of conventional ^1H -MRI and the sensitivity of contrast-enhanced ^1H - or ^{19}F -MRI are not comparable to those of PET. Hence, for future applications of MRI in the clinical assessment of plaque lesions in humans, technological innovations at multiple levels are needed, including MR rf coil development and the discovery of high-affinity amyloid ligands with efficient BBB permeability.

The AD pathology targeted by MR and PET imaging may not be confined to senile plaques. It may also be possible to image neurofibrillary tau lesions in vivo. Our preliminary investigation using tau transgenic mice indicated that the presence of neurofibrillary tangles does not overtly alter contrast in conventional ^1H -MRI and that intravenously administered FSB can robustly bind to the intraneuronal tau aggregates. Thus, it is conceivable that in the near future therapeutic approaches specific to tau pathology and the resultant neurodegeneration [15] can be evaluated by time-course studies using in vivo imaging systems.

References

- [1] Higuchi M, Lee VMY, Trojanowski JQ. Pathobiological features in neurodegenerative diseases: an overview. In: International Congress Series 1260: *The Senescence-Accelerated Mouse (SAM): An Animal Model of Senescence* (eds. Nomura Y, Takeda T, Okuma Y). Elsevier, Amsterdam (2004) pp. 69-75.
- [2] Saido TC. Overview – A β metabolism: from Alzheimer research to brain aging control. In: *A β Metabolism and Alzheimer's Disease* (ed. Saido TC). Landes Bioscience, Georgetown (2003) pp. 1-16.
- [3] Higuchi M, Lee VMY, Trojanowski JQ. Tau and axonopathy in neurodegenerative disorders. *Neuromolecular Med* 2 (2002) 131-150.
- [4] Price JL, Morris JC. Tangles and plaques in nondemented aging and "preclinical" Alzheimer's disease. *Ann Neurol* 45 (1999) 358-368.
- [5] Skovronsky DM, Zhang B, Kung MP, Kung HF, Trojanowski JQ, Lee VMY. In vivo detection of amyloid plaques in a mouse model of Alzheimer's disease. *Proc Natl Acad Sci USA* 97 (2000) 7609-7614.
- [6] Zhuang ZP, Kung MP, Hou C, Skovronsky DM, Gur TL, Plossl K, Trojanowski JQ, Lee VM, Kung HF. Radioiodinated styrylbenzenes and thioflavins as probes for amyloid aggregates. *J Med Chem* 44 (2001) 1905-1914.
- [7] Sato K, Higuchi M, Iwata N, Saido TC, Sasamoto K. Fluoro-substituted and ^{13}C -labeled styrylbenzene derivatives for detecting brain amyloid plaques. *Eur J Med Chem* 39 (2004) 573-578.
- [8] Higuchi M, Iwata N, Matsuba Y, Sato K, Sasamoto K, Saido TC. ^{19}F - and ^1H -MRI detection of amyloid- β plaques in vivo. *Nat Neurosci* 8 (2005) 527-533.
- [9] Jack CR Jr, Garwood M, Wengenack TM, Borowski B, Curran GL, Lin J, Adriany C, Grohn OH, Grimm R, Poduslo JF. In vivo visualization of Alzheimer's amyloid plaques by magnetic resonance imaging in transgenic mice without a contrast agent. *Magn Reson Med* 52 (2004) 1263-1271.
- [10] Lovell MA, Robertson JD, Teesdale WJ, Campbell JL, Markesbery WR. Copper, iron, and zinc in Alzheimer's disease senile plaques. *J Neurosci* 158 (1998) 47-52.
- [11] Poduslo JF, Wengenack TM, Curran GL, Wisniewski T, Sigurdsson EM, Macura SI, Borowski BJ, Jack CR Jr. Molecular targeting of Alzheimer's amyloid plaques for contrast-enhanced magnetic resonance imaging. *Neurobiol Dis* 11 (2002) 315-329.
- [12] Wadghiri YZ, Sigurdsson EM, Sadowski M, Elliott JI, Li Y, Scholtzova H, Tang CY, Aguinaldo G, Pappolla M, Duff K, Wisniewski T, Turnbull DH. Detection of Alzheimer's amyloid in transgenic mice using magnetic resonance microimaging. *Magn Reson Med* 50 (2003) 293-302.
- [13] Scarpini E, Scheltens P, Feldman H. Treatment of Alzheimer's disease: current status and new perspectives. *Lancet Neurol* 2 (2003) 539-547.
- [14] Klunk WE, Engler H, Nordberg A, Wang Y, Blomqvist G, Holt DP, Bergstrom M, Savitcheva I, Huang GF, Estrada S, Ausen B, Debnath ML, Barletta J, Price JC, Sandell J, Lopresti BJ, Wall A, Koivisto P, Antoni G, Mathis CA, Langstrom B. Imaging brain amyloid in Alzheimer's disease with Pittsburgh Compound-B. *Ann Neurol* 55 (2004) 306-319.
- [15] Hutton M, McGowan E. Clearing tau pathology with A β immunotherapy - reversible and irreversible stages revealed. *Neuron* 43 (2005) 293-294.